Available online at www.sciencedirect.com
ScienceDirect
Astroparticle Physics 29 (2008) 229–242
Astroparticle Physics
www.elsevier.com/locate/astropart

Detection of high-energy solar neutrons and protons by ground level detectors on April 15, 2001

Y. Muraki [a,*], Y. Matsubara [a], S. Masuda [a], S. Sakakibara [a], T. Sako [a], K. Watanabe [a,i], R. Bütikofer [b], E.O. Flückiger [b], A. Chilingarian [c], G. Hovsepyan [c], F. Kakimoto [d], T. Terasawa [d], Y. Tsunesada [d], H. Tokuno [d], A. Velarde [e], P. Evenson [f], J. Poirier [g], T. Sakai [h]

[a] *Solar-Terrestrial Environment Laboratory, Nagoya University, Furo-cho, Chikusa, Nagoya 464-8601, Japan*
[b] *Physikalisches Institut, University of Bern, Bern, CH-3012 Bern, Switzerland*
[c] *Yerevan Physics Institute, Yerevan, AM-375036, Armenia*
[d] *Department of Physics, Tokyo Institute of Technology, Meguro, Tokyo 152-8551, Japan*
[e] *Instituto Investigaciones Fisicas, Universidad Mayor de San Andres, La Paz, Casilla 8635, Bolivia*
[f] *Bartol Research Institute, University of Delaware, Newark, DE 19716, USA*
[g] *Department of Physics, University of Notre Dame, Notre Dame, IN 46556, USA*
[h] *College of Industrial Technologies, Nihon University, Narashino 275-0005, Japan*
[i] *Space Sciences Laboratory, University of California, Berkeley, 7 Gauss Way 7450, Berkeley, CA 94720, USA*

Received 17 February 2007; received in revised form 21 December 2007; accepted 31 December 2007
Available online 11 January 2008

Abstract

In association with the large solar flare of April 15, 2001, the Chacaltaya neutron monitor observed a 3.6σ enhancement of the counting rate between 13:51 and 14:15 UT. Since the enhancement was observed beginning 11 min before the GLE, solar neutrons must be involved in this enhancement. The integral energy spectrum of solar neutrons can be expressed by a simple power law in energy with the index $\gamma = -3.0 \pm 1.0$. On the other hand, an integral energy spectrum of solar protons has been obtained in the energy range between 650 MeV and 12 GeV. The spectrum can also be expressed by a power law with the power index $\gamma = -2.75 \pm 0.15$. The flux of solar protons observed at Chacaltaya (at $\geqslant$12 GeV) was already one order less than the flux of the galactic cosmic rays. It may be the first simultaneous observation of the energy spectra of both high-energy protons and neutrons. Comparing the *Yohkoh* soft X-ray telescope images with the observed particle time profiles, an interesting picture of the particle acceleration mechanism has been deduced.

PACS: 95.85.Ry; 96.60.qe; 96.60.Vg

Keywords: Solar neutron and proton; Neutron telescope; Neutron monitor; Easter event; Solar cosmic rays

1. Introduction

More than 25 years have passed since the discovery of solar neutrons by the detector onboard the *SMM* satellite [1] and detectors located on high mountains [2–4]. Initially detection of solar neutrons was a very rare event. At that time, we did not know whether or not solar neutrons were produced impulsively or produced by gradually accelerated ions. Even today, we cannot say that we understand well the particle acceleration mechanism at the sun, for example whether they are accelerated by a shock mechanism [5–9] or by a DC mechanism [10].

Our effort to collect more solar neutron events has provided partial answers to these questions. The ions are observed to be accelerated simultaneously to high energies with electrons, because when solar neutron events are observed, hard X-rays are detected [11–13]. Strong

* Corresponding author. Tel.: +81 52 789 4314; fax: +81 52 789 4313.
E-mail address: muraki@stelab.nagoya-u.ac.jp (Y. Muraki).

0927-6505/$ - see front matter © 2008 Elsevier B.V. All rights reserved.
doi:10.1016/j.astropartphys.2007.12.007

emission of hard X-rays is usually observed for a few minutes. Therefore it is natural to conclude that ions are also accelerated to high-energy within a few minutes.

However, exceptional cases are sometimes seen. Strong emissions of neutrons and hard X-rays from the sun have been observed at different times. As an example of such an event, we cite an event observed by the solar neutron telescope in Tibet on September 24, 2001 [14]. Another example is the event of September 7, 2005 which was observed by the solar neutron detectors located at Chacaltaya and Mexico [15,16]. We do not understand yet why the emission of gamma-ray lines was weak in this event. Thus, there still remain several important and interesting questions regarding solar neutron physics. We therefore plan to observe solar neutrons during the solar cycle 24.

In this paper, we describe an interesting event detected in association with the solar flare of April 15, 2001. On April 15, 2001 a strong flare was observed at the west limb of the solar surface at the position S20W85. The position of the sun was suitable for the neutron detectors located at Chacaltaya, Bolivia and Gornergrat, Switzerland and possibly at Mt. Aragats, Armenia. Ground level detectors observed a GLE (ground level enhancement) in association with this flare [17–25]. The GLE is normally defined as a cosmic ray phenomenon in association with solar flares, i.e. the counting rate of the cosmic rays increases, apparently due to the solar particles.

The event was successfully observed by the *Yohkoh* spacecraft and very beautiful pictures were taken by soft X-ray telescope (SXT) and hard X-ray telescope (HXT). The gamma-ray spectrometer (GRS) onboard *Yohkoh* also detected high-energy gamma-rays. The intensity of X-rays measured by the *GOES* satellite was X14, a very strong flare.

In association with this gigantic solar flare, the Chacaltaya neutron monitor observed a 3.6σ enhancement of the counting rate. In this paper, we will describe the results of observations made by these detectors. The plan of the paper is as follows. Our solar detectors are described in the following section. In Section 3, the general features of the event observed by different stations are reported. Then the results of the data analysis are given in Section 4. In Section 5 the acceleration mechanism is discussed using the *Yohkoh*/SXT images.

2. The solar detectors

2.1. The Chacaltaya neutron monitor

The Chacaltaya observatory is located at the altitude of 5250 m in Bolivia and includes a neutron monitor and a solar neutron counter. The latter has been in operation since 1992. The neutron monitor is a standard 12NM64. It consists of BF_3 counter tubes surrounded by polyethylene moderator, lead producer, and polyethylene reflector (total area is 13.1 m^2). "High-energy" (about 10–1000 MeV) nucleons enter the lead target, interacting with the lead nuclei. Then the "medium-energy" neutrons (1–20 MeV) are produced by the evaporation and cascade processes of the lead nuclei. Those medium-energy neutrons collide with the hydrogen atoms in the polyethylene and reduce their momentum by the collisions. Then these "low-energy" neutrons can enter into the BF_3 counter (a proportional counter) located at the center of the neutron monitor inside the lead ring. Then by the nuclear reaction with the Boron of the counter gas, $^{10}B + n \rightarrow \alpha + {}^{7}Li$, an alpha particle is produced and the proportional counter can register the entrance of a neutron. Since the electronics of the detector was designed to be sensitive only to $Z \geqslant 2e$ particles, the neutron monitor does not record the minimum ionizing particles such as relativistic muons and electrons. So a neutron monitor is an almost background free detector for secondary cosmic rays like muons and electrons and has a sensitivity to hadronic components like neutrons and protons. The detection efficiency was calculated as 10–40% by [26,27] (it depends on the energy) and calibrated with a neutron beam from the accelerator [28].

2.2. The Chacaltaya plastic neutron counter

The Chacaltaya plastic neutron counter is composed of 4 m^2 plastic scintillator with a thickness of 40 cm covered with anti-counters so that the detector can separate neutral particles from charged particles like muons, electrons and protons. Photons can penetrate the anti-counters and be converted into electron positron pairs inside the plastic scintillator. Those photons form the background for the detection of neutrons. The detection efficiency of the scintillators for neutrons was calibrated in accelerator measurements. It is approximately 30% (the efficiency is ≈8% for every 10 cm thickness of the scintillator) [29].

A good comparison of the neutron monitor and the neutron counter at Chacaltaya can be made by use of the event on September 7, 2005 [15]. In Fig. 1, we plot the respective responses. The neutron monitor recorded 95,000 additional neutrons during 10 min, while the plastic scintillation detector recorded 21,500 events for $E_n > 40$ MeV, 11,700 events for $E_n > 80$ MeV, 3000 events for $E_n > 160$ MeV and 820 events for $E_n > 240$ MeV. They are 22.6%, 12.3%, 3.2% and 0.8% of the flux detected by the neutron monitor, reflecting the energy spectrum of the arriving neutrons. We note here that the threshold energies of the third and the highest channels of the Chacaltaya plastic neutron counter have been adjusted in February 18, 2005 from 120 to 160 MeV and 160 to 240 MeV, respectively. Therefore the counting rates of these two channels are different before and after February 18, 2005.

The detection efficiencies of the plastic neutron counter for solar neutrons per unit area is estimated to be nearly equal to that of neutron monitor (≈20–30%). However, the area of the Chacaltaya neutron monitor is three times larger than the plastic neutron counter. Taking into account the difference in the acceptance of the two detec-

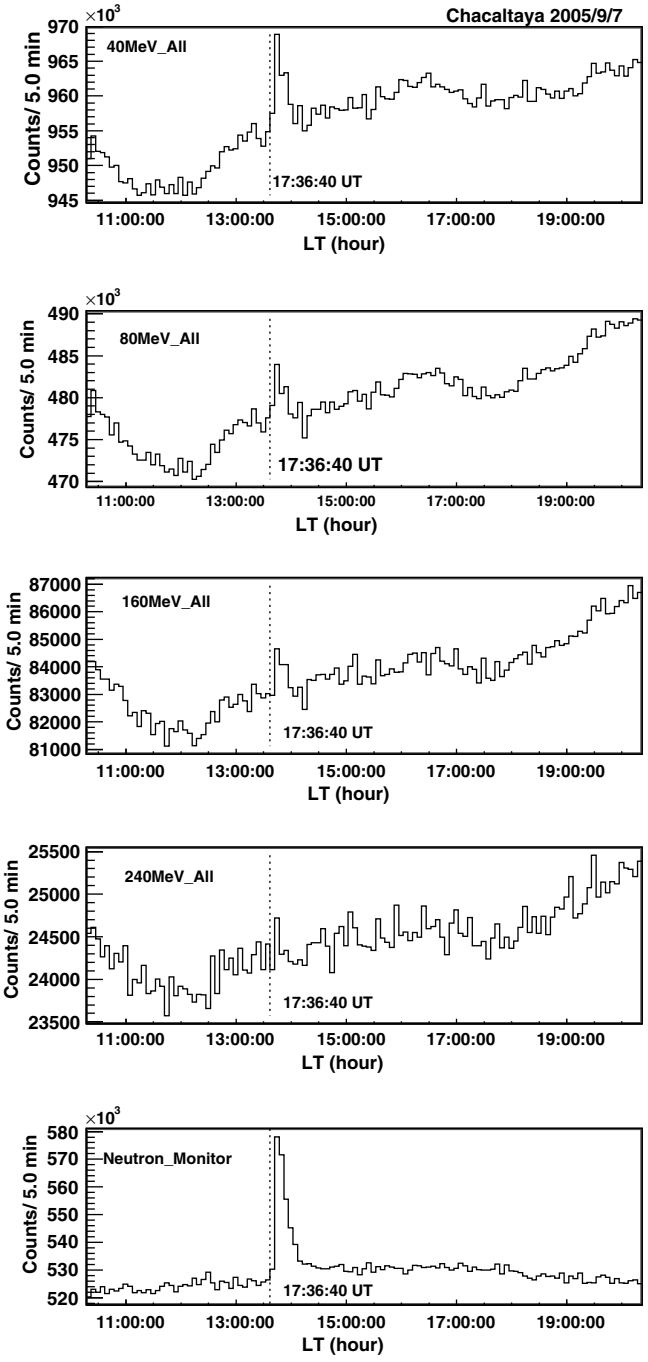

Fig. 1. The 5 min values observed by the solar neutron telescope and the neutron monitor located at Chacaltaya on September 7, 2005 event. Both plastic neutron detector and neutron monitor observed clear signals in this event. The horizontal axis corresponds to the local time in Bolivia.

tors, the counting rate of the plastic neutron counter in Chacaltaya was 22.6% of the neutron monitor. In other words, the counting rate per unit area of the plastic neutron counter was 67.8% of the neutron monitor. However, the neutron monitor usually provides us the over counting rate of an event. The over counting effect by the neutron monitor has been estimated by using actual data themselves. The fluctuation of the counting rate observed by the neutron monitor does not always show a Gaussian distribution and slightly spreads. When we divide the deviation of the counting rate from the means by 1.52, the distribution of the counting rate obtained by the Chacaltaya neutron monitor shows the Gaussian distribution. Thus, taking account of the 1.52 effect, the detection efficiencies of both detectors are expected to be nearly the same per unit area.

It is worthwhile to note here that the neutron monitor cannot determine the energy of neutrons by itself while the neutron counter can measure the minimum-energy of arriving neutrons because those neutrons collide with carbon or hydrogen targets in the plastic scintillator and produce proton tracks. The energy of the protons can be measured from the track length, i.e. it is proportional to the intensity of the light.

2.3. The Swiss neutron telescope and the Mt. Aragats plastic neutron counter

The Swiss neutron telescope at Gornergrat is composed of 4 m^2 plastic scintillators with a thickness of 40 cm. In order to veto charged particles, the plastic scintillators are surrounded by proportional counters. Details of the detector were reported by Bütikofer et al. [30] and Moser et al. [31]. The detector records the arrival directions of solar neutrons. They are binned into five directions from north to south.

The Armenian plastic neutron counter at Mt. Aragats is similar to the Chacaltaya plastic neutron counter but the thickness of the 4 m^2 plastic scintillator is 60 cm and the anti-counter is located on the top of the detector. Details can be found in another Ref. [32].

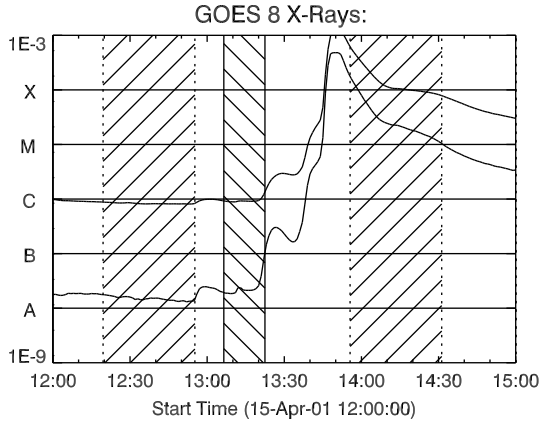

Fig. 2. The X-ray intensity time profile observed by the *GOES* satellite. The upper curve shows the wavelength band, 0.1–0.8 nm, while the lower curve shows the band, 0.05–0.4 nm. The X-ray intensity increased in three steps; at 13:28 UT (C4), 13:40 UT (M1), and 13:48 UT (X10). The shadows represent the South Atlantic Anomaly (negative slope) for the *Yohkoh* satellite and shadow of the Earth (positive slope) for the *Yohkoh* orbit, respectively. The vertical axis units are W/m^2. The levels A, B, C, M, and X refer to X-ray event levels for the 0.1–0.8 nm band.

2.4. The project GRAND-detector

GRAND is located adjacent to the University of Notre Dam, Indiana, at 86W42N with an altitude of 220 m a.s.l. Each detector station is composed of eight planes of position sensitive orthogonal wire proportional chambers which measure track angles to ±0.25° in each of two proportional planes. Vertical muons with energy above 0.1 GeV traverse a 0.7 ton steel plate in each station; 96% of the straight tracks through this steel are muons. The total muon detecting area of 64 such stations is 82 m^2. The threshold energy of the detector to primary protons is estimated to be about 30 GeV by the M.C. calculation [33] and the median-energy for primary protons is estimated as 56 GeV by the M.C. calculation [24] for galactic cosmic rays; since the index, gamma, is similar for this flare, the resulting median-energy should also be similar. At the time of the solar flare of April 15, 2001, the local time was 8:30 a.m.; thus GRAND was looking toward the direction of the interplanetary magnetic field.

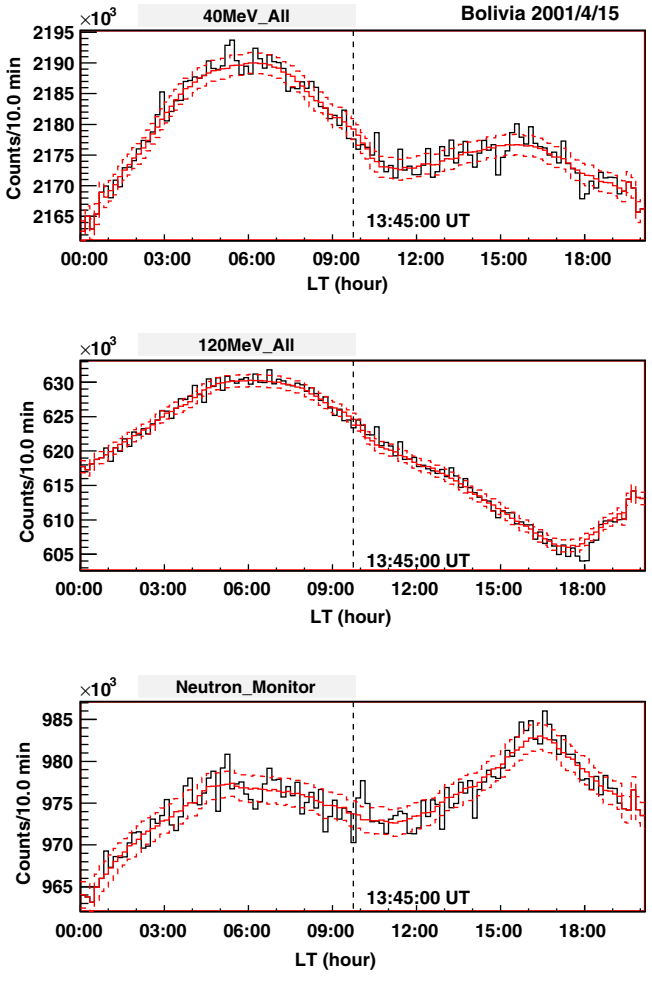

Fig. 3. Ten minutes values observed by the Chacaltaya plastic neutron detector (top and middle panel) and by the neutron monitor (bottom panel) on April 15, 2001. A typical daily variation was seen in the lowest threshold channel of the neutron counter and the neutron monitor around at 4 p.m. local time. The dotted lines correspond to the 1σ statistical fluctuations.

2.5. The Yohkoh/SXT, HXT and GRS

The *Yohkoh*/SXT records X-ray images of solar flares. The dynamic motion of coronal loops detected by *Yohkoh*/SXT has been reported elsewhere [34]. In this paper, the data of the SXT are used to understand the acceleration mechanism of particles. The detector is sensitive to X-rays in the energy range from 0.25 keV to 4.0 keV [35]. When electrons are accelerated to high energies, X-rays with shorter wavelengths beyond 10 keV are emitted. The *Yohkoh* hard X-ray telescope, HXT has four windows for different wavelengths from 10 to 100 keV [36]. The Easter flare occurred at the west limb of the sun and HXT obtained beautiful pictures showing X-ray images.

The *Yohkoh* satellite carried the gamma-ray spectrometer, GRS. The detector could record gamma-rays within the energy range between 270 keV and 100 MeV [37]. High-energy photons are emitted by high-energy electrons through Bremsstrahlung and gamma-ray lines are emitted by mechanisms inherent to the ions. In particular, the 2.223 and 4.44 MeV gamma-ray lines are well known to

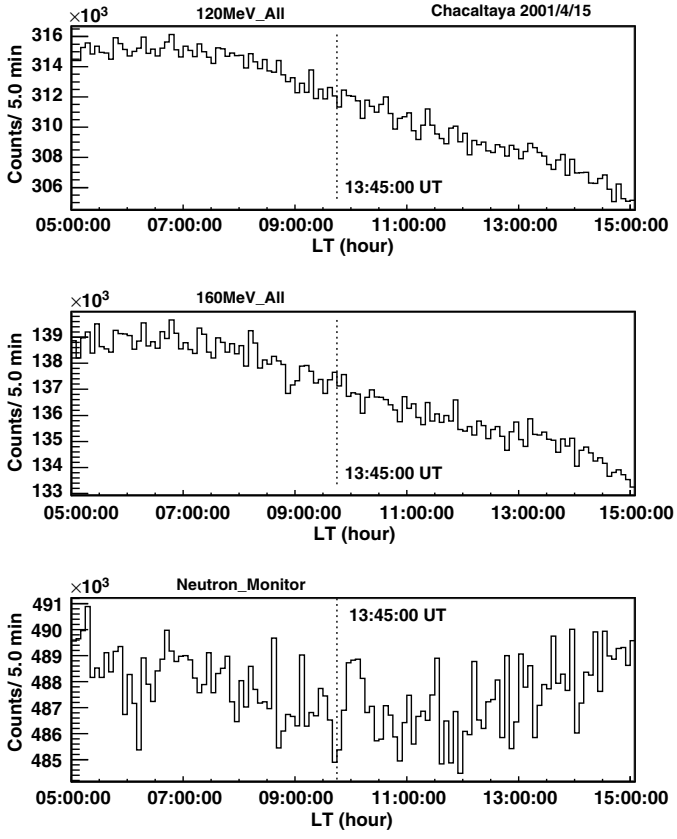

Fig. 4. Five minutes values observed by the Chacaltaya plastic neutron detector (top and middle panel) and by the neutron monitor (bottom panel) in April 15, 2001. A clear enhancement was seen in the data of the neutron monitor starting around 13:48 UT. The horizontal axis represents the local time in Bolivia.

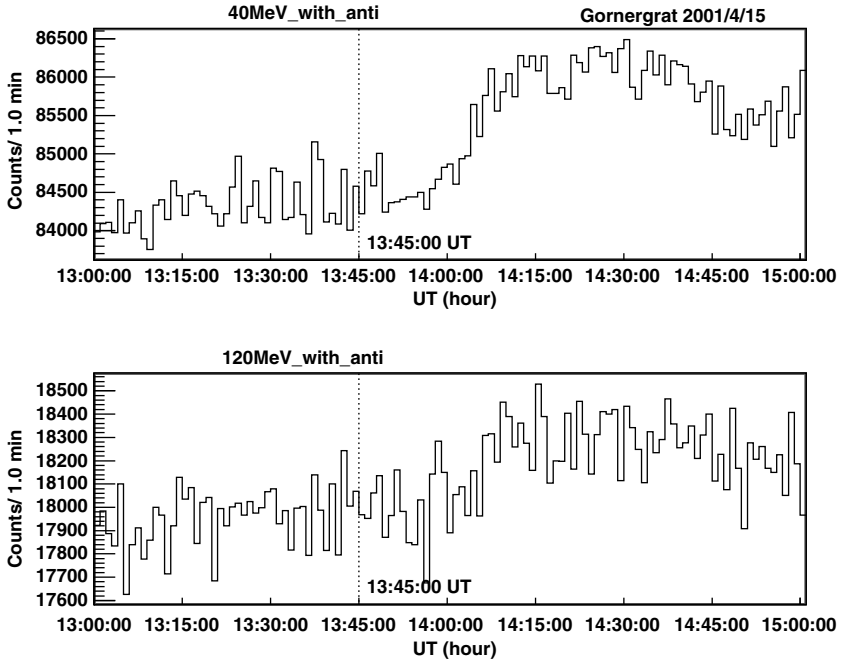

Fig. 5. The time profile of the counting rate of the neutral channel observed by the Gornergrat neutron telescope for the event on April 15, 2001. Top panel represents the intensity of neutral particles above 40 MeV and bottom panel represents the intensity above 120 MeV.

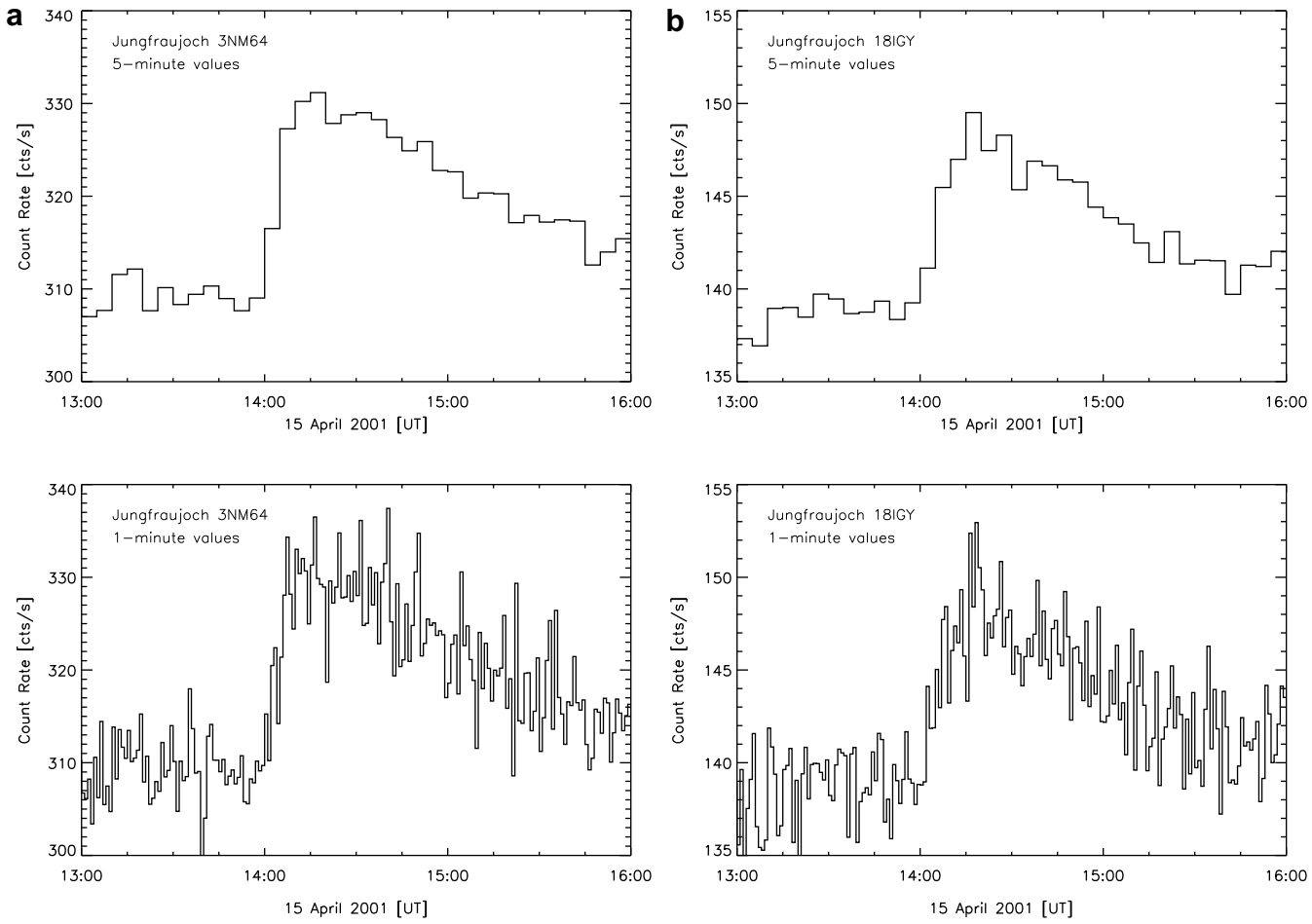

Fig. 6. The 5 and 1 min values of the neutron monitors located at Jungfraujoch. (a) The data were obtained by 3NM64 and (b) the data observed by the 18IGY neutron monitor. The altitude of the location is 3470 and 3570 m, respectively.

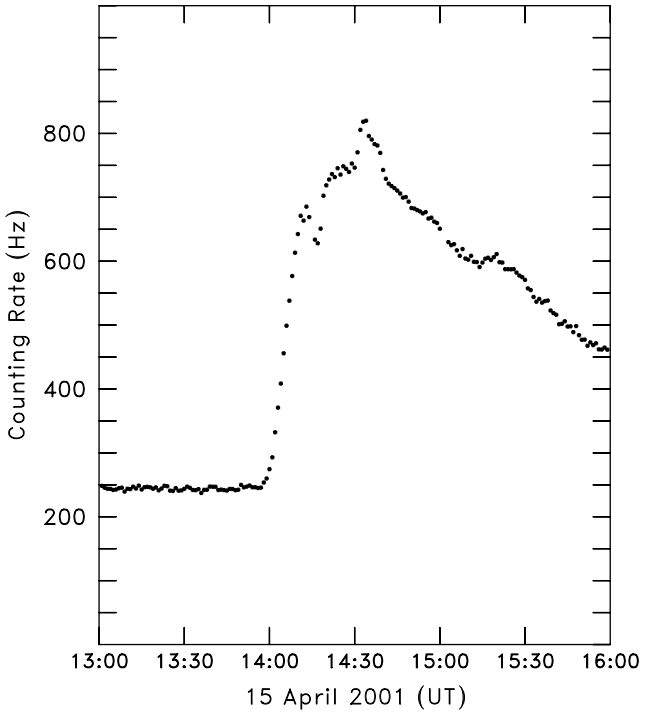

Fig. 7. The 1 min data of the neutron monitor located at the South Pole. The altitude of the South Pole is 2820 m. The data in the plot represents the data after correction for atmospheric pressure.

originate from the neutron capture line and the de-excitation line of carbon and oxygen in the solar atmosphere. Those gamma-ray lines provide evidence of ion acceleration.

3. Observation of the Easter event

3.1. X-ray observation

According to the observation of the *GOES* satellite, the flare started at 13:19 UT and reached maximum at 13:50 UT. However, as shown in Fig. 2, the flare increased in intensity by three steps from a level of C4 at 13:28 UT, to M1 at 13:40 UT, and to X10 at 13:48 UT. The X-rays increased abruptly from M4 to X10 within 3 min between 13:45 and 13:48 UT. The *Yohkoh* satellite could observe the flare from the initial stage at 13:22 UT through the maximum until 13:56 UT. The shadows shown in Fig. 2 represent the South Atlantic Anomaly of the *Yohkoh* satellite and the shadow of the Earth for the *Yohkoh* orbit.

3.2. Observations from Chacaltaya

Fig. 3 shows the 10 min time profiles observed by the Chacaltaya neutron monitor and the plastic neutron counter. The data of the neutron monitor and the plastic neutron counter with >40 MeV show a typical daily variation and the minimum value was observed around 11 a.m. local time, while high-energy parts of the plastic counter show only pressure variations [38]. As shown in Fig. 4, in the 5 min time profile of the neutron monitor, we can see a clear peak starting from 13:51 UT. However, in the data of the plastic neutron counter, only marginal (2σ level) enhancements were observed. The 5 min data of the neutron monitor tell us that the excess continued for more than 30 min, while the data of the plastic scintillator

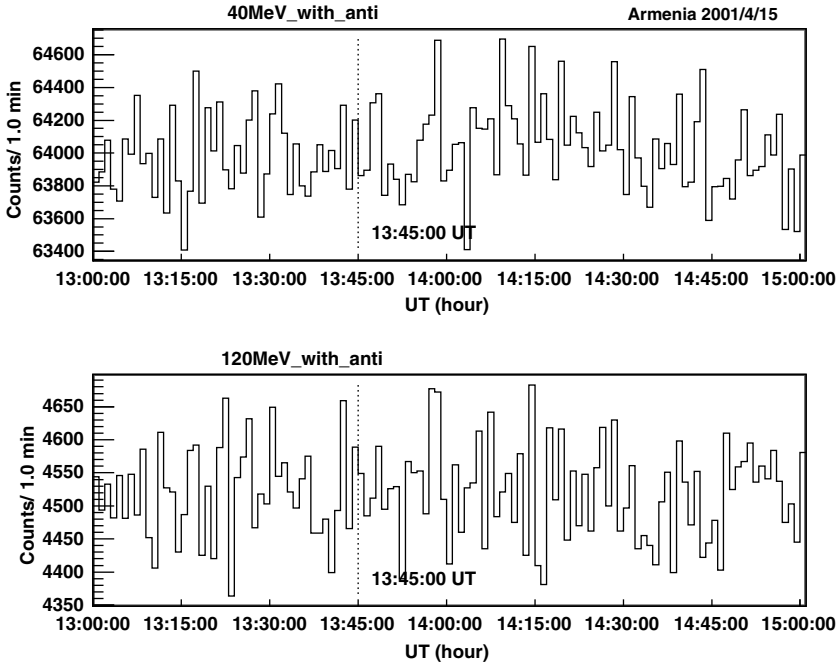

Fig. 8. The time profile of the counting rate of the neutral channel observed by the Mt. Aragats neutron counter. Top panel represents the intensity of neutral particles above 40 MeV and bottom panel represents the intensity above 120 MeV. The Mt. Aragats detector did not see the increase due to the GLE.

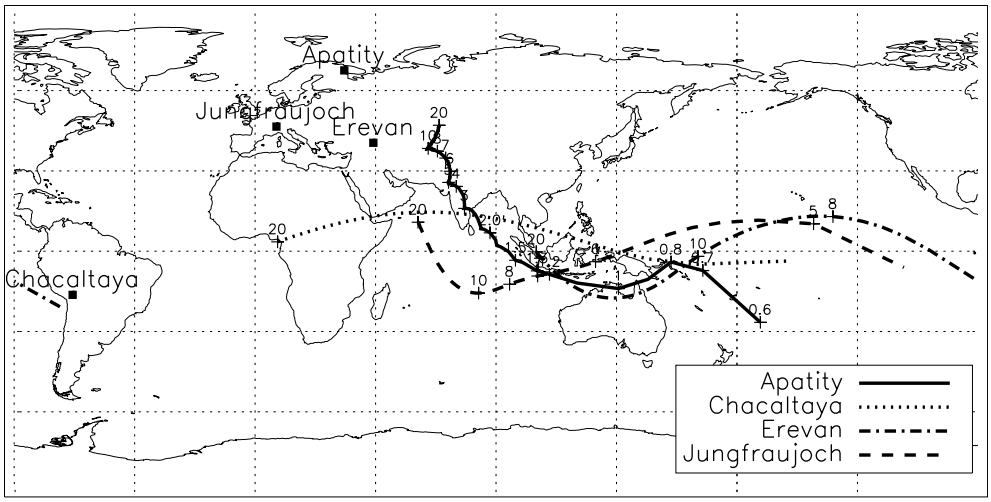

Fig. 9. Asymptotic directions of vertically incoming cosmic ray particles at the NM stations Apatity (solid line), Mt. Chacaltaya (dotted line), Aragats, Yerevan (dashed-dotted line), and Jungfraujoch (dashed line) at 13:45 UT on April 15, 2001. The numbers close to the lines give the rigidity of the particles in GV.

show an excess in the highest-energy channel ($E_n > 160$ MeV) in a 1 min interval only. The background may mask the high-energy low flux part of the signal. The statistical significance of the excess observed by the neutron monitor in the 24 min from 13:51 and 14:15 UT is 3.6σ.

3.3. Observation from Jungfraujoch and Gornergrat

In Fig. 5, we plot the time profile of the counting rate of the neutral channel recorded by the Gornergrat neutron telescope. Fig. 6 displays the 5 and 1 min values for the 3NM64 type neutron monitors and the 18IGY type neutron monitors located at Jungfraujoch. Their altitudes are 3475 and 3570 m, respectively. Fig. 6b indicates that the GLE started from 14:02 UT.

3.4. Observation from South Pole

Fig. 7 shows the neutron monitor data observed at the South Pole in the Antarctic located at 2820 m. As can be seen from Fig. 7, the increase of the counting rate started at ≈14:00 UT, nearly the same time observed by the neutron monitors at Jungfraujoch. The vertical geomagnetic cutoff rigidity for protons at Jungfraujoch and the South Pole are 4.44 and 0.09 GV [39], respectively.

3.5. Observation from Mt. Aragats

Fig. 8 represents the time profile of the neutron counter located at Mt. Aragats. No remarkable enhancement due to the GLE was seen at Mt. Aragats. We have calculated the asymptotic directions of cosmic rays arriving at selected

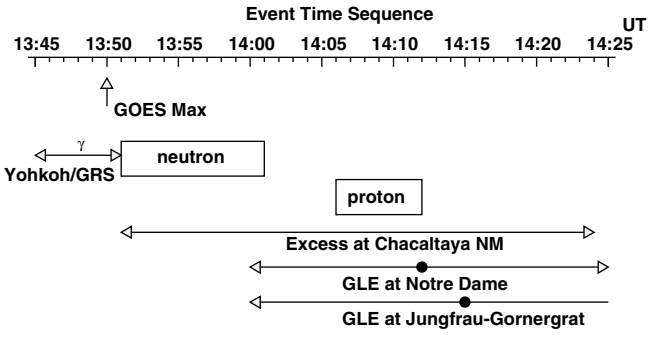

Fig. 10. The event time profile observed by each detector as a function of universal time. Following the detection of gamma-rays with energy 4–7 MeV by the *Yohkoh* GRS detector, high-energy neutrons and protons were detected by the Chacaltaya neutron monitor. The excess as a function of time used for determining the statistical significance is indicated by the box. The GLE commenced at 14:01 UT and continued for 2 h, however, the high-energy portions with energy >30 GeV continued for only 25 min. The small filled circles indicate the peak time of the GLE recorded at each station. Each time corresponds to the time at the Earth.

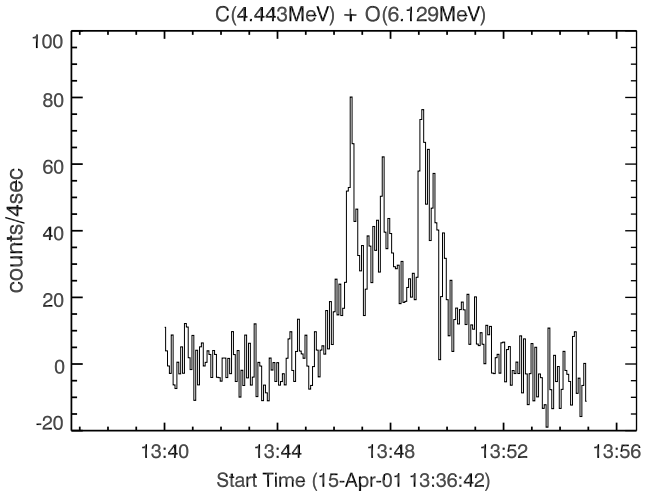

Fig. 11. The gamma-ray time profile observed by *Yohkoh*/GRS. The counting rate observed in the energy range between 4 and 7 MeV for carbon and oxygen gamma-ray lines.

neutron monitor stations. The results are shown in Fig. 9. The atmospheric depth to the sun was 719 and 808 g/cm^2 at Chacaltaya and Gornergrat, respectively, but at Mt. Aragats it was 1006 g/cm^2. According to our empirical knowledge, signals of solar neutrons in current detectors were not observed when the atmospheric depth is deeper than 800 g/cm^2 [40].

3.6. Summary of Section 3

For the Chacaltaya neutron monitor, the cutoff rigidity is estimated as 12.1 GV. The Chacaltaya neutron detectors did not see any remarkable enhancement due to "traditional" GLE that enhances rapidly and decays slowly for more than 2 h like Figs. 5–7. This suggests that the low-energy solar protons were rejected by the geomagnetic field and could not reach the Chacaltaya observatory at 5250 m. We conclude therefore that the enhancement observed by the Chacaltaya neutron monitor between 13:51 and 14:02 UT must be mainly due to solar neutrons.

4. Results of the data analysis

In this section we give results of the data analysis. The sequence of observations is shown in Fig. 10. Fig. 11 shows the time profile of the gamma-rays in the energy range of 4–7 MeV observed by the *Yohkoh*/GRS during 13:40–13:55 UT. We assume that ions were accelerated with the same time profile as gamma-rays, i.e. the ions were accelerated from 13:45 UT, as shown in Fig. 11 and particle acceleration continued until 13:51 UT, the end of strong emission of gamma-rays. Also we assume that the energy spectrum of solar neutrons can be expressed by a power law. Fig. 12 shows the reduced χ^2-values of fitting the measurements of the Chacaltaya neutron monitor by assuming a power law spectrum with indices γ in the range -3.0 to -9.0. The dependence of the reduced χ^2-value from the power index, γ, was made by fitting the measurements in the time intervals 13:45–14:15 UT and 13:48–14:06 UT. The reduced χ^2-value for the fit in the time range 13:48–14:06 UT has a minimum at $\gamma = -4.0$ (or the integral $\gamma = -3.0$).

The result of fitting the data between 13:51 and 14:06 UT with $\gamma = -4.0$ is presented in Fig. 13 by filled circles. From Fig. 13, a deviation from the fit can be seen around the peak at 14:06 UT. Therefore we have used a modified model to fit the observed data. In the solar flare of May 24, 1990, the arrival time of neutrons is clearly separated from the arrival time of protons [41,42]. However, in the flare of April 15, 2001, the time difference between arrival times of the neutrons and the protons was short. Since the flare occurred at the west limb (W85), protons arrived at the Earth rapidly. This complicates the situation. We assume from 13:51 to 14:02 UT that only neutrons are involved in the enhancement observed at Chacaltaya as shown in the box of Fig. 10. However, after 14:02 UT, high-energy protons may be included in the data. The

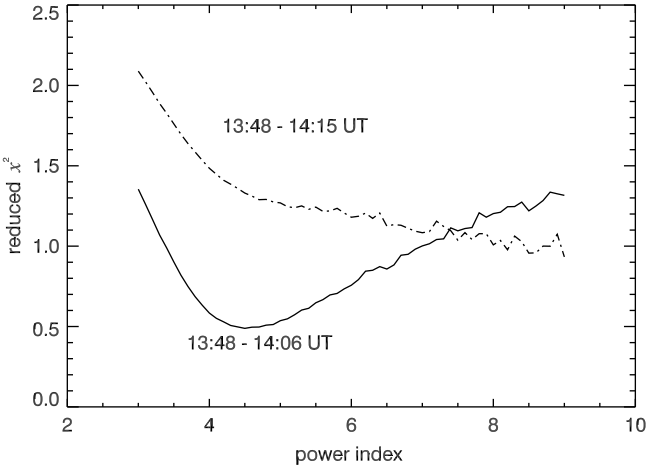

Fig. 12. The reduced χ^2-value of the fitting. When we attempt to fit the impulsive production model to the data between 13:48 UT and 14:15 UT, χ^2-values does not show a minimum (dashed-dotted line). However, when we fit the data between 13:48 and 14:06 UT, the χ^2 has a minimum value at $\gamma \sim -4.0$ (solid line).

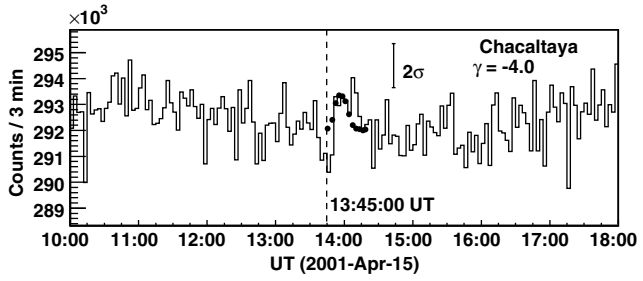

Fig. 13. The results of fitting the 3 min values of the Chacaltaya neutron monitor at the time interval between 13:51 and 14:15 UT. We have assumed that neutrons were produced with the same production time profile of gamma-rays as shown in Fig. 11. In the time 14:06–14:12 UT, another peak can be recognized in the data of the neutron monitor. This second peak may be induced by the high-energy solar protons with $E_p > 12$ GeV, since during this time the GLE was observed.

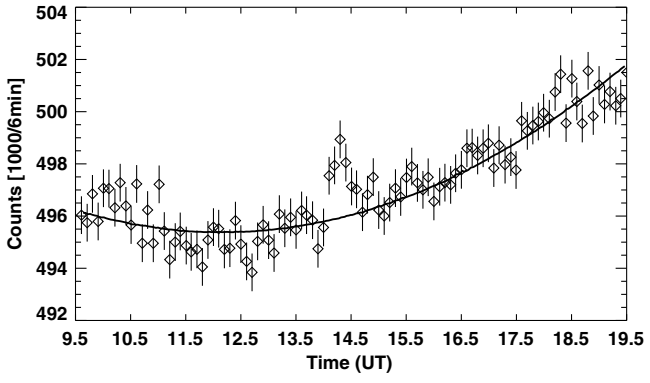

Fig. 14. The 6 min counting rates above background observed by GRAND (boxes with error bars). A 6.1σ enhancement was seen during 14:00–14:30 UT. The line represents the background. Muons produced by protons with energies above ≈20 GeV can be detected by GRAND. The median-energy for primary protons is estimated as 30 GeV.

hypothesis is strongly supported by the data obtained by GRAND as shown in Fig. 14. We attempted to separate the proton and neutron components in this time interval, since the GLE started at 14:02 UT.

According to the analysis of past neutron data by one of the authors [11], the differential production spectrum of solar neutrons can be expressed by a power law with the index $\gamma = -3.0$ to -4.0. The present result is consistent with this analysis.

We obtained the proton flux after 14:06 UT by subtracting the neutron flux from the raw data. The procedure was as follows. The event time profile was fit to the expected curve with a power law. The data points of Fig. 13 represents the expected points for neutrons. The residuals from these plots were regarded as a proton component. The number of protons is estimated to be 3500 events for 6 min during 14:06–14:12 UT. The statistical significance is 3.0σ while the statistical significance of the neutron component is 3.0σ. A multiplication factor of 1.52 has been applied to the neutrons inside the neutron monitor.

Statistical significances were determined as follows. Fig. 15a shows the 5 min values recorded by the Chacaltaya neutron monitor (bottom panel of Fig. 4) together with the fitted background (solid line) and its one sigma deviations (dashed lines). The latter were determined by allowing for the multi-counting correction factor of 1.52 described above. The result is shown in Fig. 15c. The shaded data points indicate statistical significances from 13:51 to 14:03 UT. Their significance is nearly 2σ. The four data points yield a combined excess of $\approx 4\sigma$.

A note maybe be written here. Those statistical significances were obtained using a background of 292,000 counts during 3 min. This background level was estimated by a running average for the 5 min value (Fig. 15) excluding possible peak regions. However, we could draw a background line at the level of 291,600 counts for 3 min. Then the statistical significance would be 4.0σ for neutrons and 3.7σ for protons. In this paper, we have used the more conservative value for the background.

Fig. 16 displays the integral flux of solar protons at the top of the atmosphere. The low-energy part of the flux was obtained by the *GOES* satellite. We assumed that the peak value of the *GOES* data reflects the energy spectrum of protons at the acceleration site. The observed peak

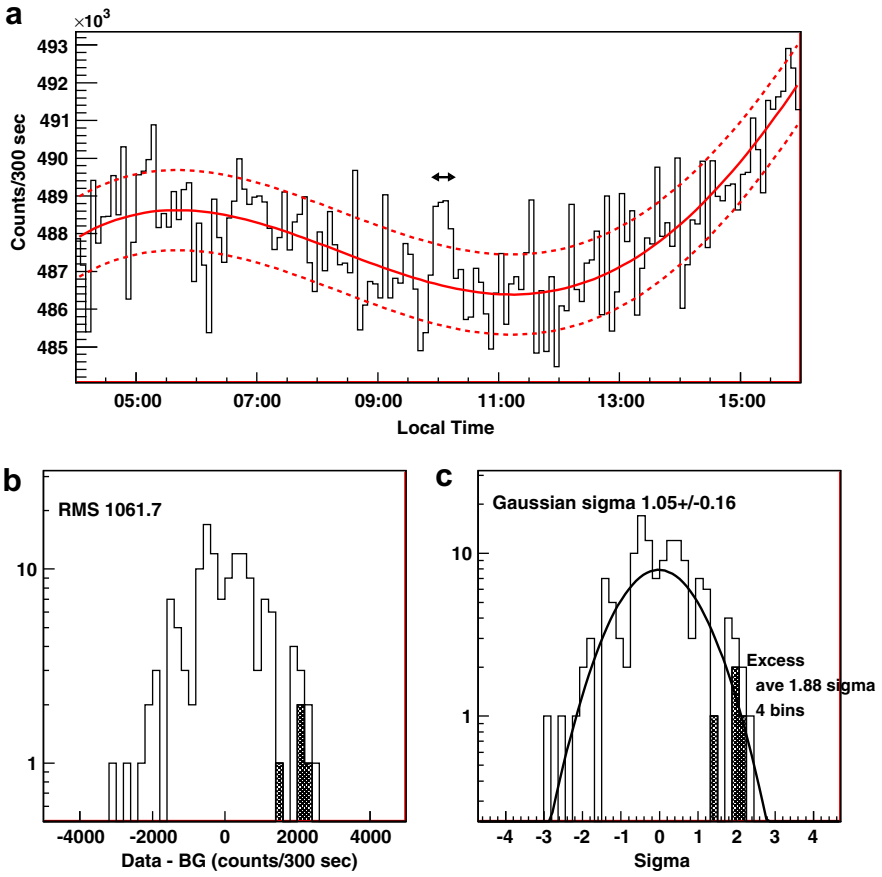

Fig. 15. (a) Five minutes values recorded by the Chacaltaya neutron monitor. The solid line shows the mean counting rate fitted by a 5th order polynomial outside the signal region. The dashed lines are one sigma limits. (b) The left panel shows the deviation of each point from the fitted background plotted on a semi-logarithmic scale. (c) The right panel shows deviations from the mean on a semi-logarithmic scale together with the Gaussian distribution (solid line). When the deviations of (b) are reduced by a factor 1.52, the deviations follow the Gaussian distribution. The four data points near 1.88σ yield a combined excess of $\approx 3.7\sigma$.

intensities for ground level detectors are plotted at their corresponding cutoff rigidities. We have used the neutron monitors located at different rigidities as a spectrometer. For the neutron monitor located at Apatity and at Jungfraujoch and Chacaltaya, we have used the multiplication factor of neutrons 1.4 and 1.52 [26], respectively. Here the error bars represent the statistical error only.

The data points for Apatity (0.65 GV), Jungfraujoch (4.44 GV) and Chacaltaya (12.1 GV) shown in Fig. 16 are obtained after the correction of the absorption effect of protons and neutrons in the atmosphere. The ratios of secondary to primary nucleons are 3×10^{-4}, 0.1 and 0.33, respectively [43–45]. We have corrected for the detection efficiency of the neutron monitors at Chacaltaya and Jungfraujoch estimated to be 30%. However, for the neutron monitor at Apatity, we have estimated it to be 20%, since the detection efficiency of the neutron monitor is lower at lower-energy (~100 MeV) [26–28]. Fig. 17 represents the integral flux of solar protons for various GLEs. The data of the Easter event are presented by black circles. It is impressive that protons were accelerated beyond 12 GeV and the flux can be expressed by a simple power law with an index of $\gamma = -2.75 \pm 0.15$ in the energy range between 650 MeV and 12 GeV. The flux of the highest-energy point observed at Chacaltaya is already one order less than the flux of the galactic cosmic rays. Since the altitude of the observatory is very high, the attenuation of solar protons was small, so we could detect the signals.

The detection of muon signals by GRAND implies that protons were accelerated beyond 30 GeV (possibly over the energy 56 GeV) in this flare [47–51]. GRAND, located adjacent to the University of Notre Dame, has recorded a 6.1σ excess in the time interval 14:00–14:30 UT shown in Fig. 14. The counting rate above background at the peak was 2900 ± 730 muons for this 6 min bin or 24 ± 6

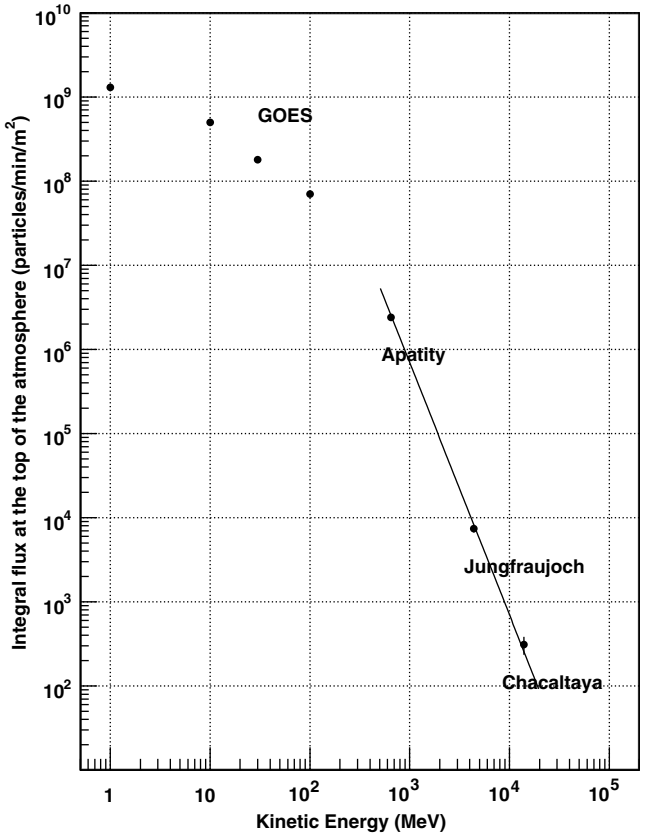

Fig. 16. The integral proton flux produced by the flare of April 15, 2001. The vertical axis represents the integral proton flux per unit m^2 and per minute. The horizontal axis represents the energy of protons. The data points correspond to the maximum flux measured by the *GOES* detector and the NM station, respectively. The maximum time of the *GOES* detector is observed on April 16 at about 3:00 UT for >1 MeV protons; and on April 15 at 19:23 UT, 16:15 UT, and 15:27 UT for protons, >10, >30 and >100 MeV, respectively; while for the neutron monitor data for Apatity 14:05 UT, for Jungfraujoch 14:18 UT and for Chacaltaya 14:06 UT, respectively. To the data points observed by the ground level detector, the rigidity at the observation point was plotted. The line corresponds to expected values from the power index $\gamma = -3.0$.

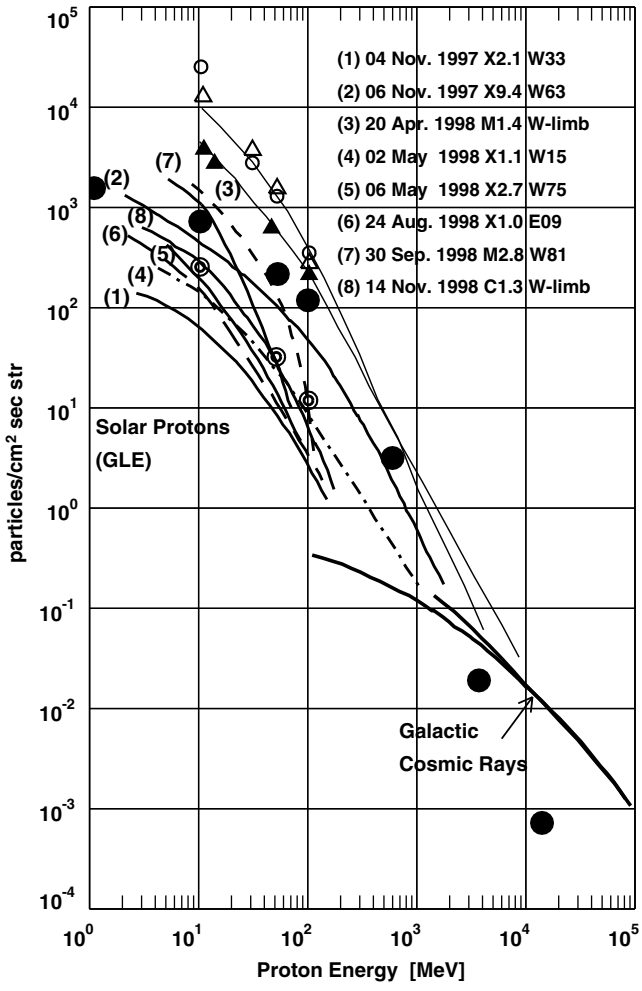

Fig. 17. The integral flux of solar protons [46]. The vertical axis is in units of particles/(cm^2 s str). The Easter event is presented by the black circles (•). The black triangles and thin line show the data observed in 1989, September 29th flare (X9.8). The open round mark and thin line corresponds to the data of the Bastille day event of 2000 (X5.7). The double circle (◎) and the open triangle (△) represent the data on April 18, 2001 flare (C2.2) and November 8, 2000 flare (M7.4), respectively.

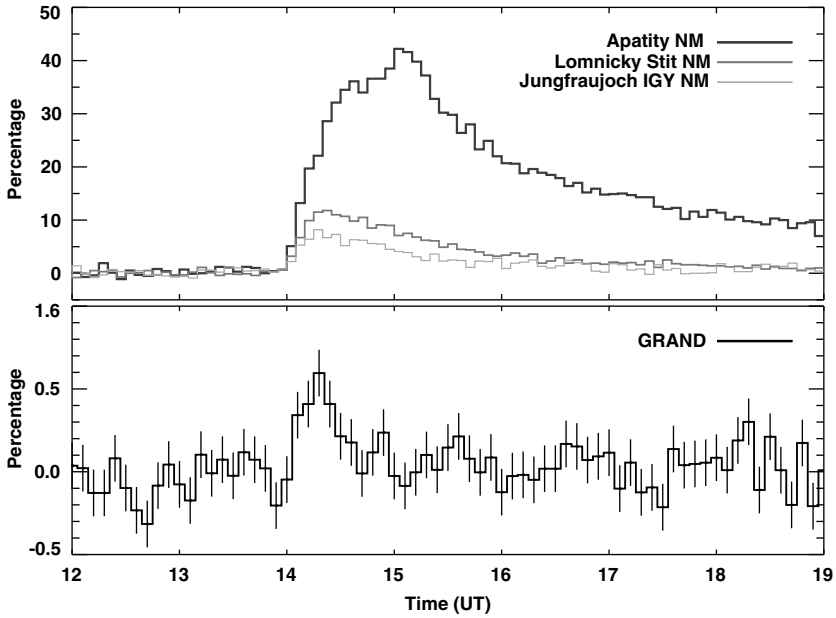

Fig. 18. The relative count rates of the neutron monitor stations Apatity, Lomnicky Stit, and Jungfraujoch and of the proportional wire chamber array of the project GRAND during the time interval 1200–1900 UT on 15 April 2001 are plotted. The excess of the GRAND experiment was small (about 0.5%) whereas it was significantly higher in the count rates of the neutron monitor stations, e.g. over 40% in the 5 min values of the station Apatity. Therefore, GRAND excesses were plotted on a different scale in the bottom panel.

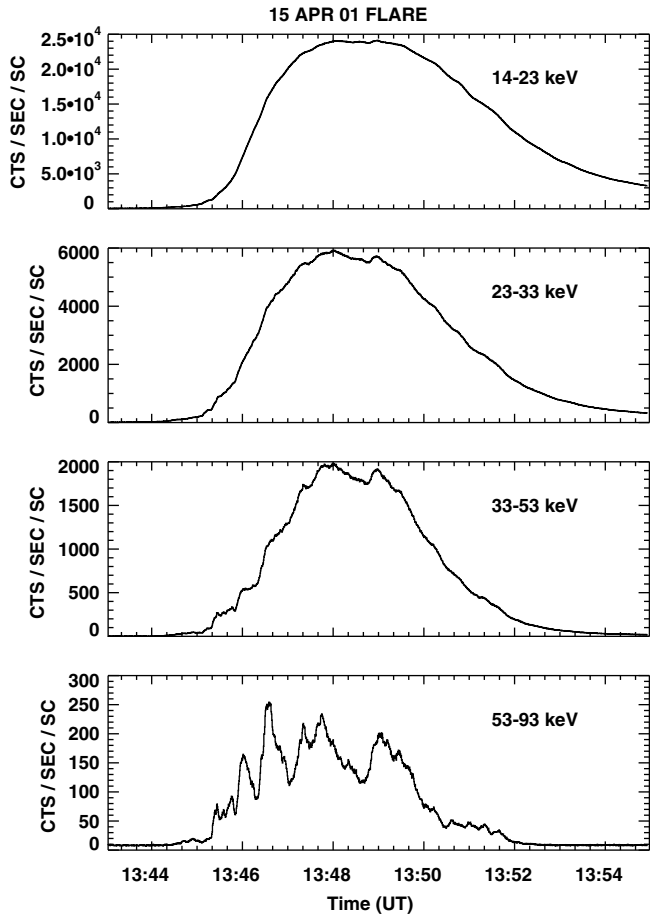

Fig. 19. The time profile of the *Yohkoh*/HXT, where the emission of the hard X-ray started at 13:44 UT on April 15, 2001. A spiky feature of the X-ray emission can be seen in the highest channel.

protons/min/m^2 for the threshold energy of 30 GeV where GRAND response function is 0.5 muon/proton [24]. For this energy of the incoming protons, the flux is estimated (the data was divided by 0.5). The shape of the time profile is similar to that of the Chacaltaya neutron monitor. The observed flux of particles at GRAND is near a straight line projection of the lower-energy points on this logarithmic plot of Fig. 17. It may be the first time the energy spectra of both high-energy protons and neutrons have been measured simultaneously, though there are a number of reports on the energy spectra of GLEs (protons) [46]. In Fig. 18, the excesses of GLEs recorded at several northern hemisphere stations are plotted. The excess shown for GRAND is very small in comparison with the other GLEs. For this

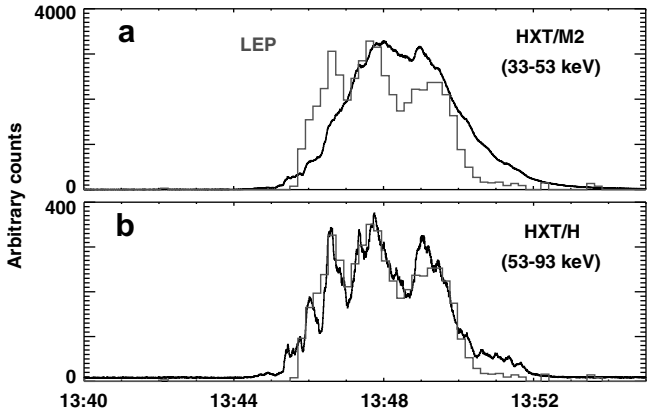

Fig. 20. Hard X-ray data observed by the *Geotail* satellite (grey) with data by *Yohkoh* (black).

reason, the data of GRAND are plotted by the different scale in Fig. 18 (bottom panel).

In closing this section, we will note a few comments on the earlier works on this event. Bieber et al. have analyzed the data obtained by the Spaceship Earth network and obtained a result that protons were accelerated to ≈GeV by a CME-driven shock wave [52]. Now neutrons are found in the data of the Chacaltaya neutron monitor. Therefore at least some part of protons must be accelerated in the magnetic loops near the solar surface and those protons must hit the solar atmosphere from the top as they moved in a downward direction. The injection time of those protons to the solar surface must be between 13:45 and 13:51 UT when the gamma-ray lines were observed by the *Yohkoh*/GRS.

We cannot conclude from our analysis whether or not protons were accelerated to high energies (>10 GeV) within the CME-driven shock waves. However, it is sure that protons are accelerated beyond $\geqslant 1$ GeV as predicted by [52]. Since the Chacaltaya neutron monitor observed proton

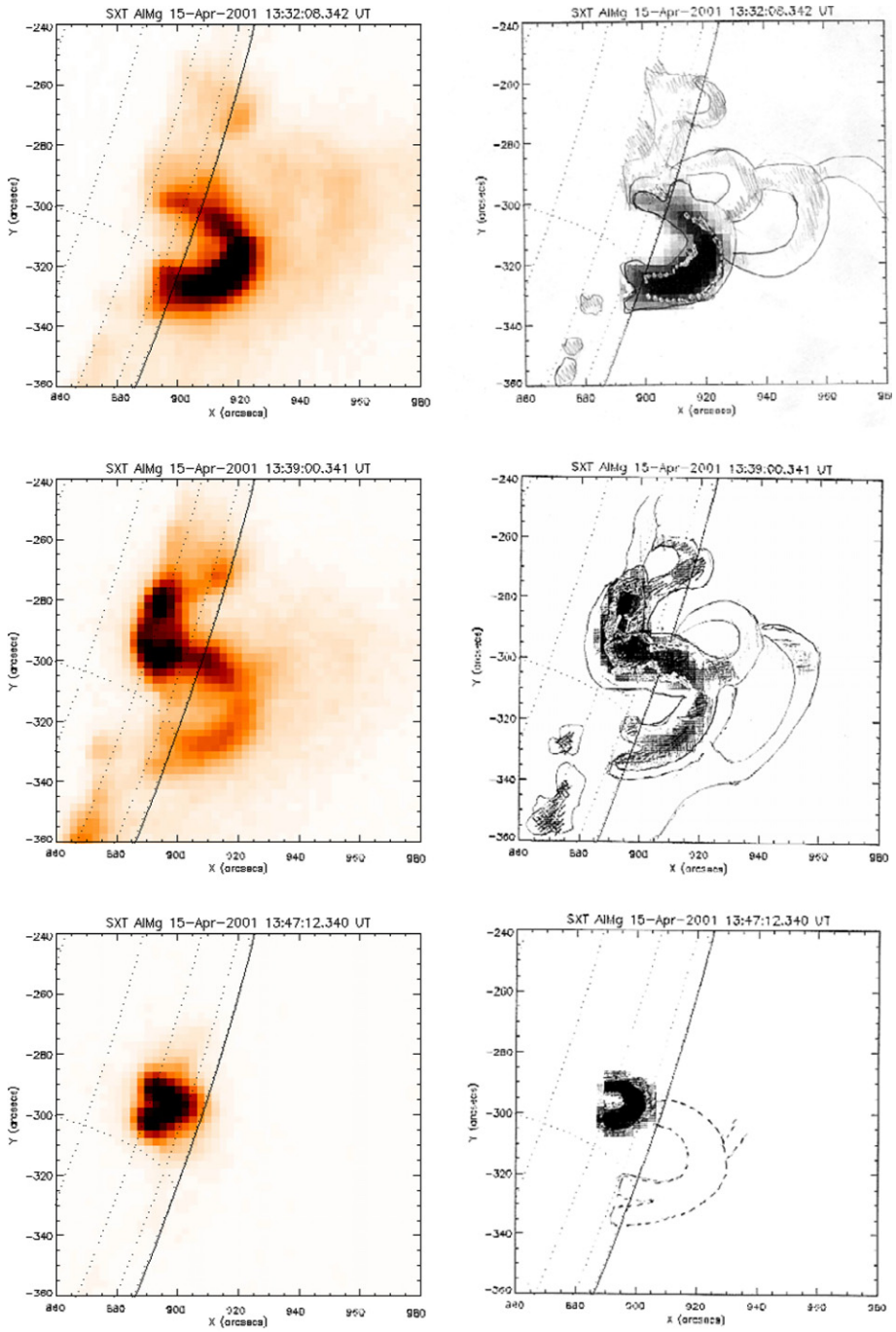

Fig. 21. Dynamical features of the corona loops observed by the SXT telescope of the *Yohkoh* in association with the large flare (left side panels). The sketches of the SXT images are shown on the right side. From the top to the bottom, the panel represents the dynamical motion of loops at C4 stage (left, 13:32 UT), M1 stage (middle, 13:39 UT) and X6 stage (bottom 13:47 UT), respectively.

components from 14:06 to 14:12 UT with 3.0σ statistical significance in coincidence with the GLE, protons must be accelerated over 12 GeV (probably beyond 30 GeV) in this flare. However, it is not clear whether those particles were accelerated by using a CME-driven shock [19,52]. Because as will be noted in the next section, the magnetic loop around 13:46–13:51 UT was NOT open towards the outer space.

5. Beautiful images observed by the *Yohkoh* detectors

Fig. 19 represents the time profile of HXT, where the emission of the hard X-rays started at 13:44 UT. Fig. 20 shows the hard X-ray data observed by the *Geotail* satellite [53]. The emission was quite notable at 13:45 UT and at 13:46:30 UT the intensity had the first peak. The second and the third peaks can be seen at 13:47:45 UT and 13:49 UT. The hardest channel (H, 53–93 keV) shows a quite spiky structure, so the particle acceleration occurred during 5 min from 13:45 to 13:51 UT [19]. The slides on the left of Fig. 21 shows the images taken by using the *Yohkoh*/SXT telescope. In Fig. 22, dominant emission of hard X-rays can be seen at three points of the loop, the foot points and at the top point. It looks like a typical Masuda flare [54]; however, the top of the loop was connected with another loop that was dominant at the time of the M1 flare. It was not open to outer space.

When we observe the flare from the initial stage, an interesting fact has been found. On the right side of Fig. 21, sketches of the dynamical behaviors of the loop are shown. Fig. 21 tells us that the loop used for the acceleration of particles is different at each stage and is different for the C4, M1 and X10 levels. The acceleration occurred in different loops and reached the maximum intensity as X14 in this event. The large flare occurred by three steps, hop(C4), step(M1) and jump(X10).

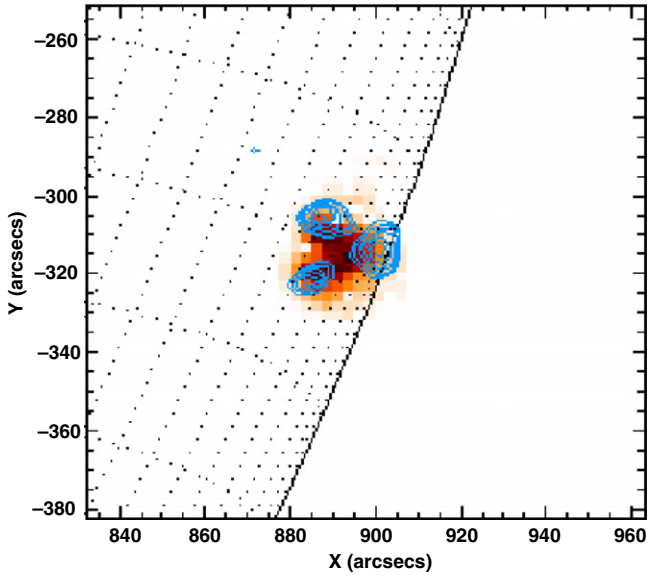

Fig. 22. The positions of hard X-rays are shown by the circle on the SXT image. The data were taken at the maximum time of the flare, 13:47 UT, when the level of X-rays reached X14.

This three-step acceleration example is not a universal feature at the sun. In most large flares, the flare abruptly and impulsively increases its intensity within a few minutes. We find another good example of the three-step acceleration in the flare of November 28, 1998 [55]. The further study of this type of particle acceleration may resolve the particle acceleration mechanism on the solar surface.

6. Summary and conclusion

On April 15, 2001, a large solar flare was observed near the west limb of the sun (the 'Easter flare'). Its position was S20W85. In association with this flare solar neutrons were observed by the Chacaltaya neutron monitor. They were produced contemporaneously with the gamma-ray lines at 13:45–13:51 UT. We conclude that protons were accelerated during this period. The energy spectra of the emitted protons and neutrons follow a power law with indices $\gamma = -2.75 \pm 0.15$ (proton integral) and $\gamma = -3.0 \pm 1.0$ (neutron integral), respectively.

The flux of high-energy protons with energies exceeding 12 GeV was an order of magnitude less than the flux of galactic cosmic rays. This rendered their detection by the GLE neutron monitor a difficult task. Such detection is probably only possible in extremely large solar flares, such as the one observed on September 29, 1989.

Acknowledgements

The authors acknowledge Prof. Philip Yock of Auckland University in NZ and Dr. Michael R. Moser of Bern University for carefully reading the manuscript and providing many valuable and useful comments. The authors also thank Bartol Research Institute of the University of Delaware for providing us their data and one of the authors (P.E.) thanks the National Science Foundation. Apatity and Lomnicky Stit neutron monitor data were kindly provided by the Polar Geophysical Institute of the Russian Academy of Sciences (PGI, Apatity) and Institute Experimental Physics of the Slovakia Academy of Science. The work of the University of Bern is supported by Swiss National Science Foundation, Grant 200020–113704. K.W.'s work is supported by the JSPS Postdoctoral Fellowships for Research Abroad.

References

[1] E.L. Chupp et al., Astrophys. J. 263 (1982) L95.
[2] E.L. Chupp et al., in: Proceedings of the 18th International Cosmic Ray Conference, vol. 10, 1983, p. 334.
[3] E.L. Chupp et al., Astrophys. J. 318 (1987) 913.
[4] Yu.E. Efimov, G.E. Kocharov, K. Kudela, in: Proceedings of the 18th ICRC, vol. 10, 1983, p. 276.
[5] R. Ramaty, R.J. Murphy, Space Sci. Rev. 45 (1987) 213.
[6] Y. Ohsawa, J. Sakai, Astrophys. J. 313 (1987) 440.

[7] M. Hoshino, J. Arons, Y.A. Gallant, A.B. Langdon, Astrophys. J. 390 (1992) 454.
[8] S. Tsuneta, T. Naito, Astrophys. J. 495 (1998) L67.
[9] M. Ohyama, K. Shibata, Adv. Space Res. 26 (2000) 461.
[10] Y.E. Litvinenko, Astrophys. J. 462 (1996) 997.
[11] K. Watanabe, Doctoral Thesis, Nagoya University, 2005 (also in: Proceedings of the Cosmic-Ray Research Section of Nagoya University, vol. 46 (2)).
[12] K. Watanabe et al., Astrophys. J. 592 (2003) 590.
[13] K. Watanabe et al., Astrophys. J. 636 (2006) 1135.
[14] T. Sako et al., in: Proceedings of the 28th ICRC, vol. 6, 2003, p. 3175.
[15] T. Sako et al., Astrophys. J. 651 (2006) L69.
[16] J.F. Valdés-Galicia et al., Nucl. Instr. Meth., Phys. Res. A 535 (2004) 656.
[17] E.G. Cordaro, M. Storini, E.F. Olivares, in: Proceedings of the 27th ICRC, 2001, p. 3368.
[18] W.F. Dietrich, A.J. Tylka, in: Proceedings of the 28th ICRC, vol. 6, 2003, p. 3291.
[19] A.J. Tylka et al., in: Proceedings of the 28th ICRC, vol. 6, 2003, p. 3305.
[20] L.I. Miroshnichenko et al., in: Proceedings of the 28th ICRC, vol. 6, 2003, p. 3321.
[21] J.W. Bieber et al., in: Proceedings of the 28th ICRC, vol. 6, 2003, p. 3397.
[22] E.V. Vashenyuk et al., in: Proceedings of the 28th ICRC, vol. 6, 2003, p. 3401.
[23] S.W. Kahler, G.M. Simnett, M.J. Reiner, in: Proceedings of the 28th ICRC, vol. 6, 2003, p. 3415.
[24] C. D'Andrea et al., in: Proceedings of the 28th ICRC, vol. 6, 2003, p. 3423. See also <http://www.nd.edu/(tilde)grand>.
[25] S.N. Karpov et al., in: Proceedings of the 28th ICRC, vol. 6, 2003, p. 3427.
[26] C.J. Hatton, in: J.G. Wilson, S.A. Wouthuysen (Eds.), Proceedings, Elementary Particle Physics and Cosmic Rays, vol. 1, North-Holland, Amsterdam, 1971, p. 1.
[27] J.M. Clem, L.I. Dorman, Space Sci. Rev. 93 (2000) 335.
[28] S. Shibata et al., Nucl. Instr. Meth., Phys. Res. A 463 (2001) 316.
[29] H. Tsuchiya et al., Nucl. Instr. Meth., Phys. Res. A 463 (2001) 183.
[30] R. Bütikofer et al., in: Proceedings of the 27th ICRC, vol. 8, 2001, p. 3053.
[31] M.R. Moser et al., in: Proceedings of the 28th ICRC, vol. 6, 2003, p. 3215.
[32] A. Chilingarian et al., in: Proceedings of the 28th ICRC, vol. 6, 2003, p. 3445.
[33] J.N. Capdeville et al., in: Proceedings of the 30th ICRC, in press.
[34] J. Sato et al., Montana State University & The Institute of Space and Astronautical Science, 2003, p. 336.
[35] S. Tsuneta et al., Solar Phys. 136 (1991) 37.
[36] T. Kosugi et al., Solar Phys. 136 (1991) 17.
[37] M. Yoshimori et al., Solar Phys. 136 (1991) 69.
[38] L.I. Dorman, Cosmic Rays – Variations and Space Explorations, North-Holland Publishing Company, 1974.
[39] L.I. Dorman, Cosmic Rays in the Earth's Atmosphere and Underground, Kluwar Academic Publishers, London, 2004.
[40] E.O. Flückiger et al., Int. J. Mod. Phys. A 20 (2005) 6646.
[41] Y. Muraki, S. Shibata, R. Ramaty, N. Mandzhavidze, X.-M. Hua (Eds.), High Energy Solar Physics, AIP Conf. Proc. 374, AIP, Greenbelt, MD, 1996, p. 256.
[42] H. Debrunner, J.A. Lockwood, J. Ryan, Astrophys. J. 409 (1993) 822.
[43] S. Shibata, J. Geophys. Res. 99 (1994) 6651.
[44] H. Menjo, private communication, 2006.
[45] J.N. Capdeville, Y. Muraki, Astropart. Phys. 11 (1999) 335.
[46] L.I. Miroshnichenko, Solar Cosmic Rays, Kulwar Academic Publishers, 2001.
[47] M. Alania et al., in: Proceedings of the 28th ICRC, vol. 6, 2003, p. 3573.
[48] D. Cattani et al., in: Proceedings of the 28th ICRC, vol. 6, 2003, p. 3577.
[49] S.N. Karpov et al., in: Proceedings of the 28th ICRC, vol. 6, 2003, p. 3457.
[50] O.C. Allkofer, in: M.M. Shapiro (Ed.), Composition and Origin of Cosmic Rays, D. Reidel Publishing Company, 1983.
[51] P.K.F. Grieder, Cosmic Rays at Earth, Elsevier Science B.V., The Netherlands, 2001.
[52] J.W. Bieber et al., Astrophys. J. 601 (2004) L103.
[53] Y. Takei et al., in: Proceedings of the 28th ICRC, vol. 6, 2003, p. 3223.
[54] S. Masuda et al., Nature 371 (1994) 495.
[55] Y. Muraki et al., Astropart. Phys. 28 (2007) 119.